

# HYDRODYNAMICS OF OCEAN PIPELINES

Susumu YOSHIHARA, Shozo TOYODA,

Katta VENKATARAMANA and Yorikazu AIKO

(Received May 31, 1993)

## Abstract

This paper describes the preliminary experimental studies on the current forces acting on cylindrical models in a steady flow, corresponding to the cases of similar but rigid and large diameter pipelines in real seas. The models were placed in a circulating water channel horizontally and normal to the direction of current flow. The strains in the models were recorded using the strain gauges from which fluid forces in the horizontal and vertical direction were obtained. The drag coefficient, the lift coefficient and the Strouhal number were also calculated and are shown against the Reynolds number.

## 1. Introduction

Marine pipelines are used for various purposes such as for transporting offshore products to onshore terminals, for carrying cables, for discharging waste in deep waters, as under-water passageways and so on. Therefore their behaviour under environmental forces has attracted wide interest. Bokain and Geoola (1987) studied the behaviour of an elastically mounted circular cylinder having vibrations restricted to a plane normal to the incident flow and concluded that the flexible cylinder may undergo either vortex-resonance, a galloping, or a combination of both. Fredsoe and Hansen (1987) investigated the lift forces acting on pipes with or without a small gap between the pipe and the sea bed and showed that the theoretical expressions can be used to predict the lift forces satisfactorily. Shankar et al (1987) determined experimentally the wave force coefficients for marine pipelines. Verley et al (1988) suggested a new hydrodynamic force model, called the wake model, for the prediction of fluid forces on seabed pipelines and showed that their model overcomes the deficiencies of the conventional Morison equation. Two effects included explicitly in the new force model, related to the wake behind the pipeline and the time dependence of the force coefficients, were supported by measurements. Chiew (1991) studied the changes in the flow pattern around horizontal circular cylinders immersed in shallow open-channel flows with different gap openings between the cylinder and the bed. He observed that the low flow depth causes backup of the upstream flow depth due to choking of the flow. This phenomenon causes the occurrence of a weir-flow condition at the cylinder, where a large drawdown forms. The net result is the increase in the drag force. Changes to both the drag and the lift forces on the cylinder for varying flow depth and gap size combinations were measured and the reasons for these changes were discussed.

Most of the above studies deal with the pipelines located on the sea bed or near the sea bed where the emphasis has been placed on scour effects. But in some situations pipelines may be far above the sea bed. This paper investigates the fluid forces on such pipelines placed well-above the

sea bed but well-below the free surface. The study also examines the variations in the fluid force as the position of the cylinders normal to the flow change.

## 2. Experimental setup

Experiments were carried out in the circulating water channel of the Faculty of Fisheries of Kagoshima University. The measuring section of this channel is 6m in length, 2m in width and 1m in depth with a maximum water velocity of 2 m/sec.

Considering the size of the water channel available for the measurements, it was decided to use hollow cylindrical pipes made of poly-vinyl chloride(p.v.c) as experimental models. Two types of models were considered for the study. First type was a single pipe(Model 1) and the second type consisted of two pipes held together side-by-side(Model 2). Figure 1 shows the experimental set up for Model 1. Experiments were carried out for two cases of Model 1 i.e., diameter = 7.5cm , 20cm . In the case of Model 2, the diameter of each of the two pipes was fixed as 7.5cm , but experiments were conducted for different inclinations of the model with respect to the flow direction i.e., the angle  $\theta$  between the flow direction and the line joining the axis of the two pipes was varied. Experiments were carried out for  $\theta = 0^\circ, 15^\circ, 30^\circ, -15^\circ$  and  $-30^\circ$ .

The central portion of the pipe was cut and a measuring section, as described below, was inserted tightly into the pipe and then the pipe was attached rigidly to steel frames and lowered into the water channel.

When same loads are applied at points of distance from the center of a simply supported beam, the bending moment is equal between those points. Using this principle, two circular plates were inserted at the center between the outer pipe and the measuring section. These plates transfer the fluid loading from the outer pipe to measuring section. Four strain gauges were attached at the two mutually perpendicular positions on the measuring section. Thus it was made possible to measure the horizontal and vertical components of fluid forces on the pipes.

Figure 2 is the photo of the measuring section with strain gauges attached. Figure 3 shows the operation of inserting the circular plates on each side of the measuring section. Figure 4 shows the

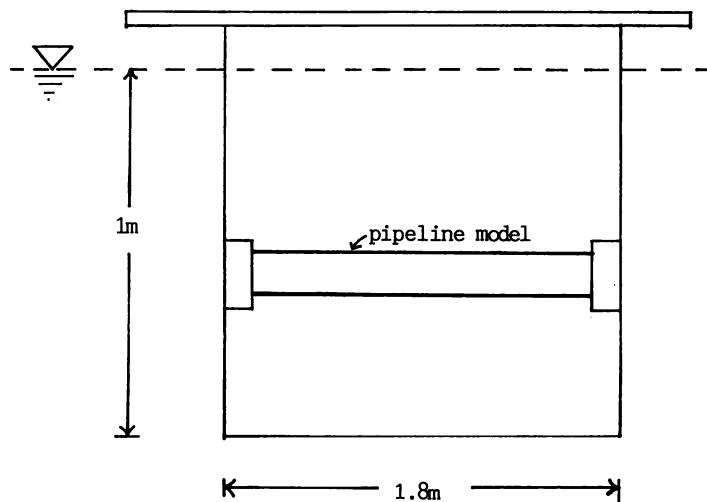


Figure 1 Experimental setup

assembling of the model. The measuring section is being tightly inserted into the pipe. Figure 5 shows the assembled model. It is being lowered into the water channel in Figure 6. Figure 7 is a snapshot of the model set in the water channel.

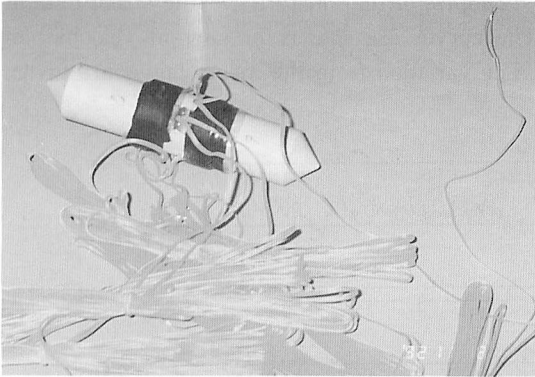


Figure 2 Photo of measuring section with strain gauges

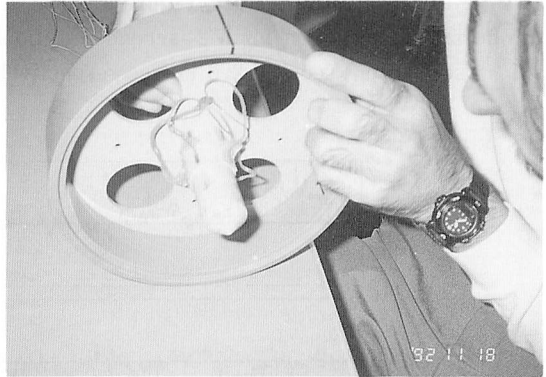


Figure 3 Inserting circular plates between the outer pipe and the measuring section



Figure 4 Assembling of the model

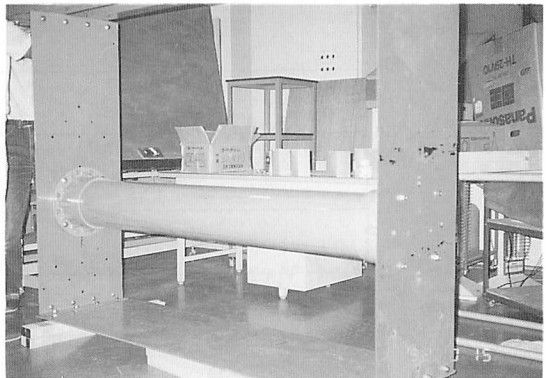


Figure 5 Photo of an assembled model

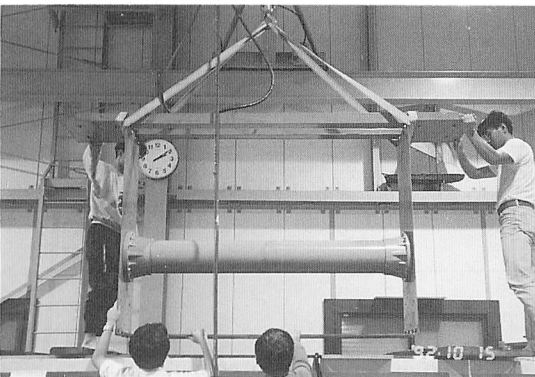


Figure 6 Lowering the model into water channel

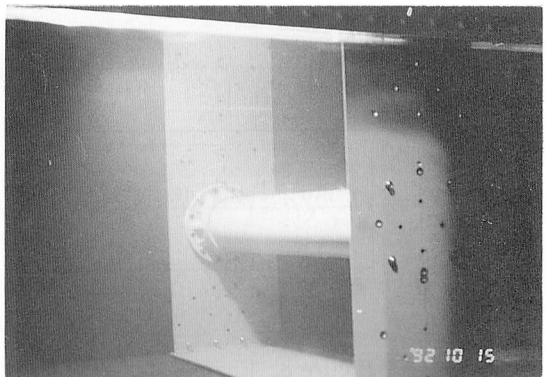
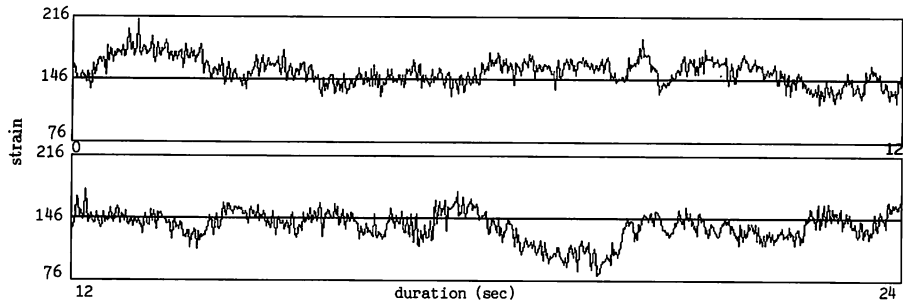


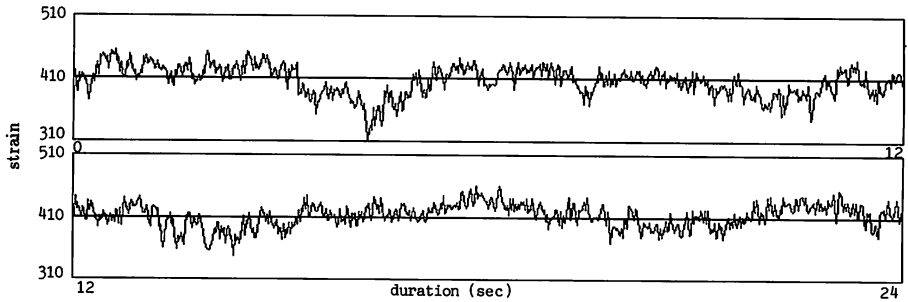
Figure 7 Snapshot of the model set in the water channel

### 3. Results

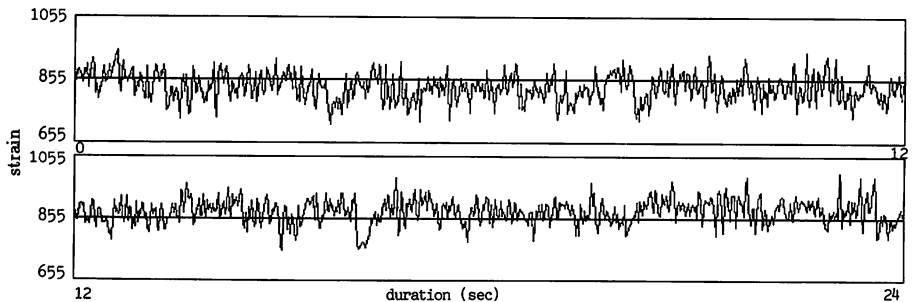
The experiments were conducted for current velocities ranging from 0.1 m/sec to 2 m/sec at 0.1 m/sec intervals. The strain data was recorded for about 40 seconds under flow conditions for each value of the current velocity. The recorded data was digitized using analog-digital converter and the time step was 0.2 sec. Figure 8 shows the examples of time histories of the strain data in the horizontal direction for a 24-second duration. The curves are shown for current velocities of 0.5 m/sec, 1.0 m/sec and 2.0 m/sec respectively. The variation from the mean values are given.



(a) current velocity = 0.5m/sec



(b) current velocity = 1.0m/sec



(c) current velocity = 2.0m/sec

Figure 8 Examples of time histories of strain in horizontal direction  
(Model 1, pipe diameter = 7.5cm)

As the current velocity increases the strain also becomes larger and more chaotic, as expected. Figure 9 shows the example of time histories of the strain data in the vertical direction. The variation in the strain for low current velocities is relatively periodic and the period may be dependent upon the eddy shedding frequency. When the flow velocities are higher, the flow is turbulent and the variation in the strain becomes random and chaotic.

The relationship between the strains and the forces inducing them were deduced from a simple static calibration test. Then, from the mean values of the fluid-induced strains, fluid forces were

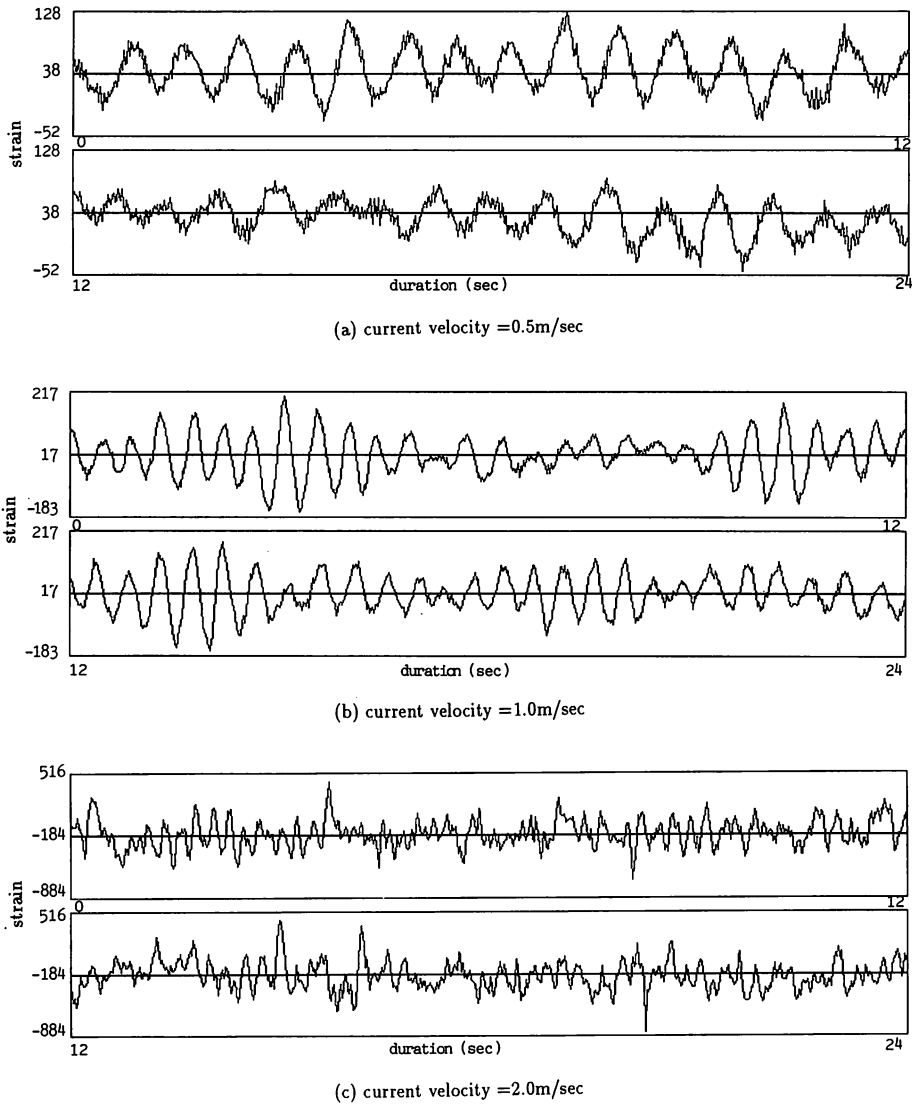


Figure 9 Examples of time histories of strain in vertical direction (Model 1, pipe diameter = 7.5cm)

calculated. Figure 10 shows the fluid forces for the case of Model 1. The mean values of the horizontal component of the fluid forces i.e., the drag force and the vertical component of the fluid forces i.e., the lift force are plotted against current velocities. Note that each value of the fluid force was deduced from the average value of the strain data for the 40-second duration. The results are shown for two cases of Model 1 i.e., pipe diameter of 7.5cm and 20cm . As expected, drag forces increase generally nonlinearly with the current velocity and also with the increase in pipe diameter. The variation in the drag force is relatively straightforward, but lift force changes more randomly as current velocities increase for the 20cm pipe indicating complex flow patterns and high of turbulence around the pipe. Figure 11 shows the fluid forces for Model 2. Four sets of force data i.e., corresponding to the horizontal(drag) and vertical(lift) forces on the pipes on the upstream side as well as on the downstream side are plotted against current velocities. The results are given for different angles of incidence  $\theta$  i.e., different angles between the flow direction and the line joining the center-line of two pipes. The drag forces generally increase with the increase in the angles of incidence because it offers more resistance to fluid flow. Also forces on the upstream pipe are larger than those on the downstream pipe.

The measured values of the forces in the above figures indicate the complexity of the flow pattern around the ocean pipelines which may depend on various factors such as eddies and other forms of turbulence, relative roughness, body orientation, proximity effects, parameters of the kinematics of the flow field, etc. It is common practice to represent these uncertainties using hydrodynamic coefficients. A coefficient  $C_d$  corresponding the drag force  $F_d$  and a lift coefficient  $C_l$  corresponding to the lift force  $F_l$  can be calculated from the normal drag and lift equations:

$$F_d(\text{or } F_l) = \frac{1}{2} C_d(\text{or } C_l) \rho A u^2 \tag{1}$$

where  $A$  is the projected area of the pipe,  $\rho$  is the mass density of water and  $u$  is the velocity of current. Figure 12 shows the values of the drag coefficient  $C_d$  plotted against the Reynolds number  $Re$ . The values follow a pattern observed generally for vertical cylinders in unidirectional flows. Figure 13 shows the values of the lift coefficient  $C_l$  plotted against the Reynolds number. The values show large scatter, the general tendency decreasing with the increase in Reynolds number is clear.

Figures 14 and 15 show the values of the drag coefficient  $C_d$  and the lift coefficient  $C_l$  respectively plotted against the Reynolds number  $Re$  for Model 2 which consists of two pipes held

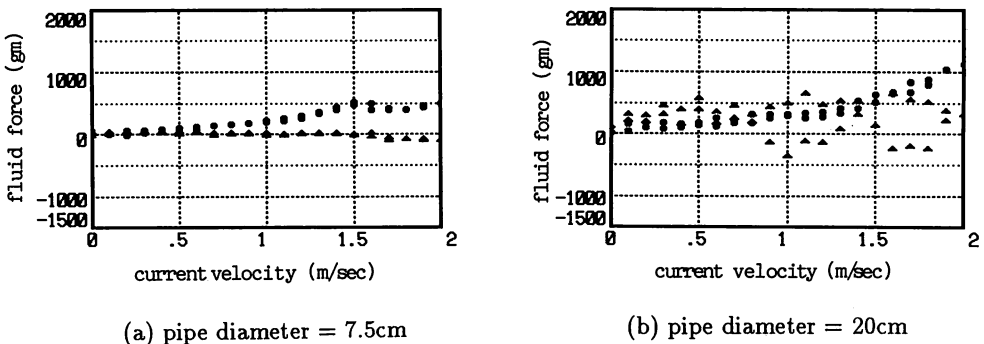


Figure 10 Fluid forces on Model 1 (• drag force; ▲ lift force)

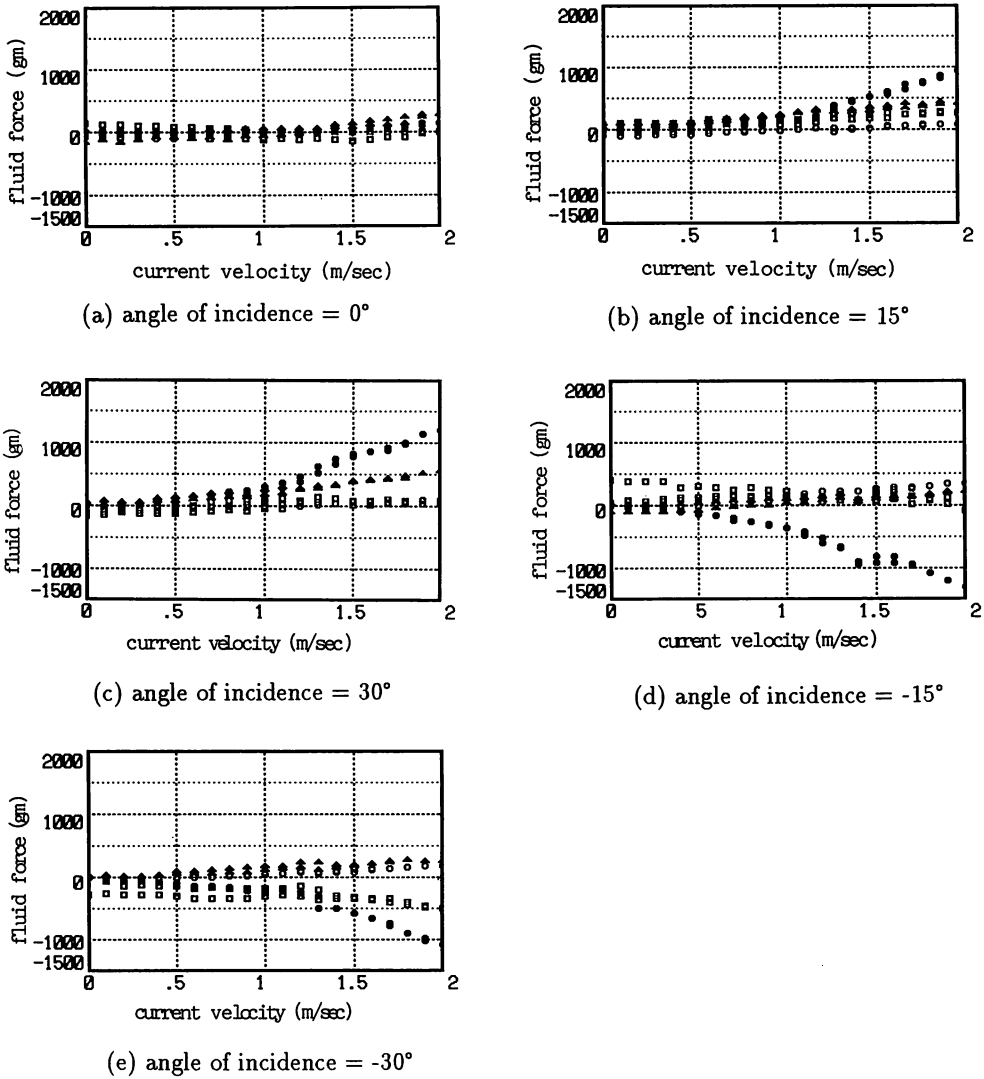
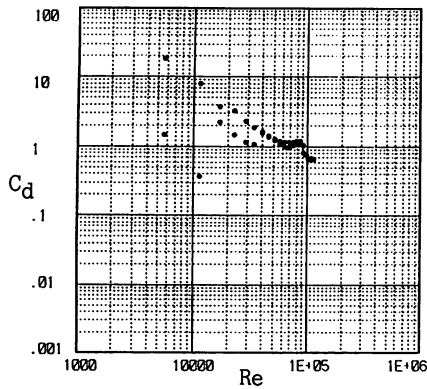


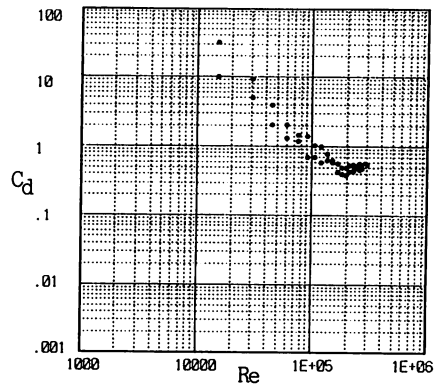
Figure 11 Fluid forces on Model 2  
 (upstream pipe : • drag force; ▲ lift force)  
 (downstream pipe : □ drag force; ○ lift force)

together. The distribution of the values of the coefficients varies with the angle of incidence and the values are different from those corresponding to Model 1 which consists of a single pipe. When two pipes are held together, as in the case of Model 2, the fluid loading on the upstream pipe and the downstream pipe vary and there are also interacting effects between these pipes. Therefore the force distribution and hence the values of the coefficients show different distribution. But the general trend of the values with the Reynolds number is the same as for single pipe of Model 1.

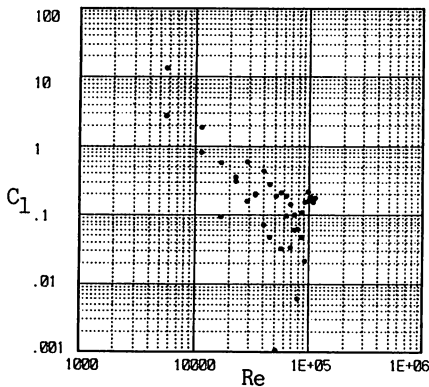
For steady flows past pipelines due to a current, the main measure of the frequency of lift forces is the Strouhal number  $S$  which is a function of the eddy shedding frequency. In the present study, the time histories



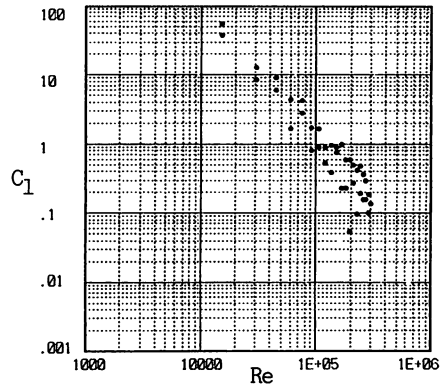
(a) pipe diameter = 7.5cm



(b) pipe diameter = 20cm

Figure 12 Drag coefficient  $C_d$  (Model 1)

(a) pipe diameter = 7.5cm



(b) pipe diameter = 20cm

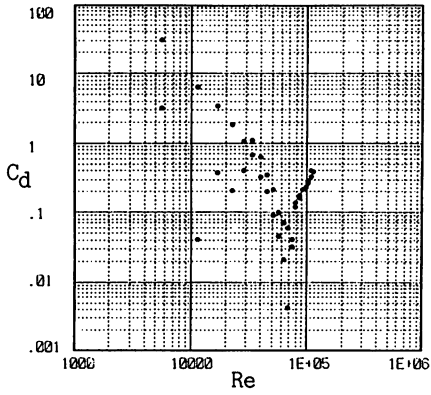
Figure 13 Lift coefficient  $C_l$  (Model 1)

of strains in the vertical direction were analyzed Fast Fourier Transform and frequencies corresponding to maximum amplitudes were located. Assuming that these correspond to eddy shedding frequencies at each current velocity, Strouhal number was calculated. Figure 16 shows this Strouhal number plotted as a function of Reynolds number for Model 1 i.e., for the case of single pipe model. The values are relatively constant for the range of the Reynolds number for small diameter pipe indicating regular shedding. For the large diameter pipe, the Strouhal number dips which indicates the approach of critical flow domain.

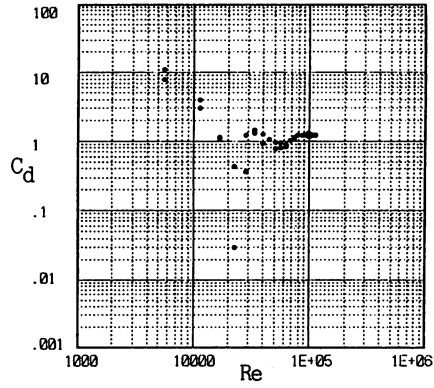
#### 4. Conclusions

A laboratory study on the hydrodynamic forces on ocean pipelines in steady current flow has been carried out. It is found that the drag force generally increases with flow velocity as expected.

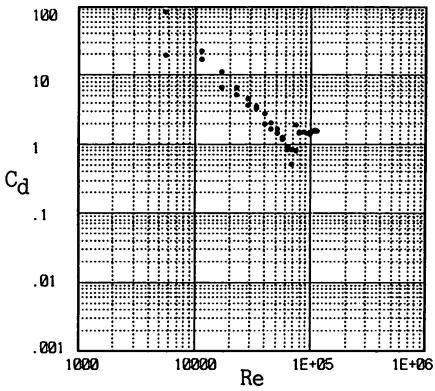




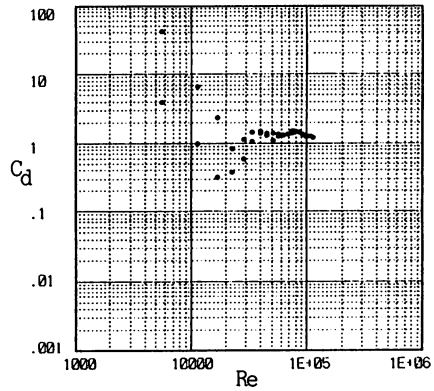
(a) angle of incidence = 0°



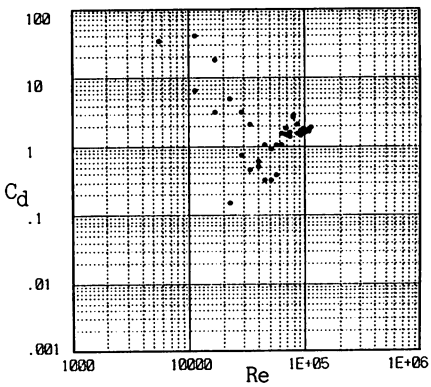
(b) angle of incidence = 15°



(d) angle of incidence = -15°

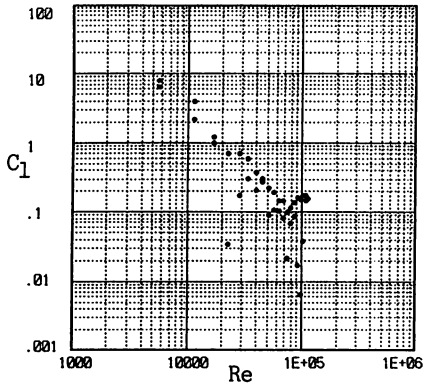


(c) angle of incidence = 30°

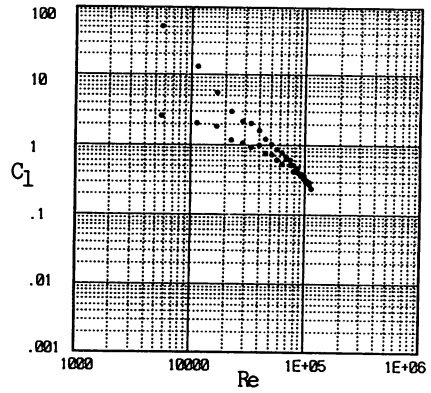


(e) angle of incidence = -30°

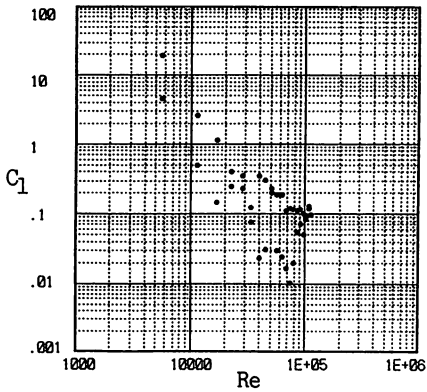
Figure 14 Drag coefficient  $C_d$  (Model 2)



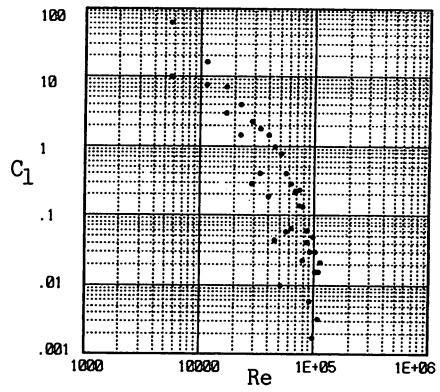
(a) angle of incidence = 0°



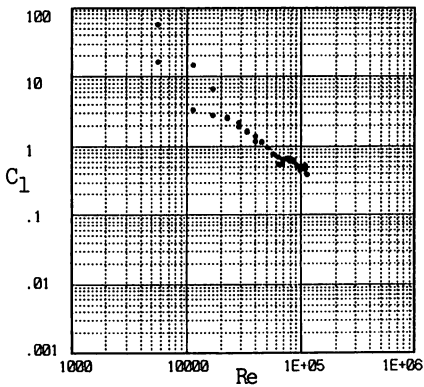
(b) angle of incidence = 15°



(c) angle of incidence = 30°



(d) angle of incidence = -15°



(e) angle of incidence = -30°

Figure 15 Lift coefficient  $C_l$  (Model 2)

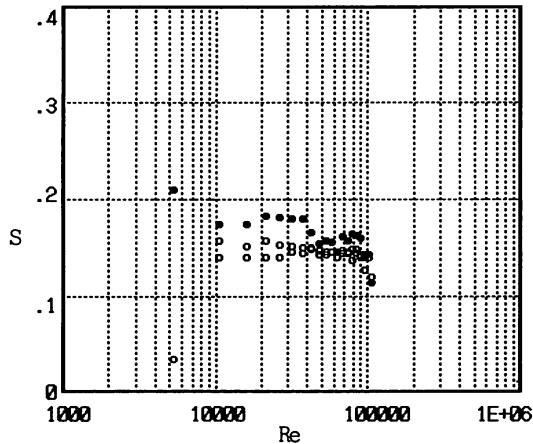


Figure 16 Strouhal number  $S$  (Model 1)  
 (○ pipe diameter = 7.5cm ; ● pipe diameter = 20cm)

The variation of lift force is more complex and is significantly affected by the eddies and other forms of turbulence around the models. For Model 2 which consists of two pipes held together, the fluid forces are greater on the upstream side. The forces are also influenced by the orientation of the pipelines with respect to flow. The values of the hydrodynamic coefficients and the Strouhal number are generally similar to the results for vertical cylinders in uniform flows.

#### Acknowledgements

Mr Shoichiro Tamae and Mr Seiichiro Ishizaka, undergraduate students, helped in carrying out the laboratory experiments.

#### References

- 1) Bokain, A. and F. Geoola (1987) :Flow-induced vibrations of marine risers, *J. Waterway, Port, Coastal and Ocean Eng.*, ASCE, 113 (1) ,pp. 22-38.
- 2) Chiew, Y. (1991) :Flow around horizontal circular cylinder in shallow flows, *J. Waterway, Port, Coastal and Ocean Eng.*, ASCE, 117 (2) ,pp. 120-135.
- 3) Fredsoe, J. and E.A. Hansen (1987) : Lift forces on pipelines in steady flow, *J. Waterway, Port, Coastal and Ocean Eng.*, ASCE, 113 (2) ,pp. 139-155.
- 4) Shankar, N.J., H. Cheong and K. Subbiah (1988) :Wave force coefficients for submarine pipelines, *J. Waterway, Port, Coastal and Ocean Eng.*, ASCE, 114 (4) ,pp. 472-486.
- 5) Verley, R.L., K.F. Lambrakos and K. Reed (1989) : Hydrodynamic forces on sea bed pipelines, *J. Waterway, Port, Coastal and Ocean Eng.*, ASCE, 115 (2) ,pp. 190-204.